electronic reprint

CRYSTALLOGRAPHIC COMMUNICATIONS

ISSN: 2056-9890
journals.iucr.org/e

Spontaneous enantiomorphism in poly-phased alkaline salts of tris(oxalato)ferrate(III): crystal structure of cubic $NaRb_5[Fe(C_2O_4)_3]_2$

O. E. Piro, G. A. Echeverría and E. J. Baran

Acta Cryst. (2018). E**74**, 905–909

Acta Cryst E CRYSTALLOGRAPHIC COMMUNICATIONS

ISSN 2056-9890

Spontaneous enantiomorphism in poly-phased alkaline salts of tris(oxalato)ferrate(III): crystal structure of cubic $NaRb_5[Fe(C_2O_4)_3]_2$

O. E. Piro,[a] G. A. Echeverría[a]* and E. J. Baran[b]

[a]Departamento de Física, Facultad de Ciencias Exactas, Universidad Nacional de La Plata and IFLP(CONICET), C.C. 67, 1900 La Plata, Argentina, and [b]Centro de Química Inorgánica (CEQUINOR), Facultad de Ciencias Exactas, Universidad Nacional de La Plata, C.C. 962, 1900 La Plata, Argentina. *Correspondence e-mail: geche@fisica.unlp.edu.ar

Received 2 February 2018
Accepted 30 May 2018

Edited by W. T. A. Harrison, University of Aberdeen, Scotland

Keywords: absolute crystal structures; spontaneous resolution of enantiomorphs; sodium and rubidium salt of tris(oxalato)ferrate(III).

CCDC references: 1563459; 1563458

Supporting information: this article has supporting information at journals.iucr.org/e

We show here that the phenomenon of spontaneous resolution of enantiomers occurs during the crystallization of the sodium and rubidium double salts of the transition metal complex tris(oxalato)ferrate(III), namely sodium penta-rubidium bis[tris(oxalato)ferrate(III)], $NaRb_5[Fe(C_2O_4)_3]_2$. One enantiomer of the salt crystallizes in the cubic space group $P4_332$ with $Z = 4$ and a Flack absolute structure parameter $x = -0.01$ (1) and its chiral counterpart in the space group $P4_132$ with $x = -0.00$ (1). All metal ions are at crystallographic special positions: the iron(III) ion is on a threefold axis, coordinated by three oxalate dianions in a propeller-like conformation. One of the two independent rubidium ions is on a twofold axis in an eightfold coordination with neighbouring oxalate oxygen atoms, and the other one on a threefold axis in a sixfold RbO_6 coordination. The sodium ion is at a site of D_3 point group symmetry in a trigonal–antiprismatic NaO_6 coordination.

1. Chemical context

Chirality is the structural property by which a molecule or ion cannot be superposed upon its mirror image through translation and proper rotation operations. This concept along with the related ones of chiral crystal structures and space groups is discussed by Flack (2003). Chirality is at the core (among other research areas) of the not yet understood origin of the biomolecular asymmetry of life (Meierhenrich, 2008), enantioselective chemical reactions (Knowles, 2001; Noyori, 2001; Sharpless, 2001), biological activity of pharmaceuticals (Nguyen *et al.*, 2006) and in the design of multifunctional solid-state materials endowed with optical activity and long-range magnetic order (Coronado *et al.*, 2003) and also in the understanding of the physical properties of chiral liquid crystals and their tailoring for applications in opto-electronic devices (Goodby, 1998; Coles, 1998).

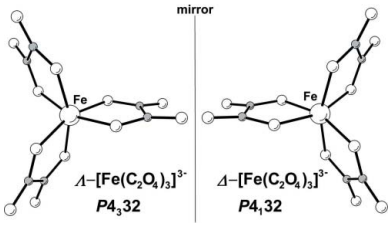

While attempting to crystallize the rubidium salt of the tris(oxalato)ferrate(III) transition metal complex, one of the preparations segregated into a poly-phased crystal system. It contained the intended $Rb_3[Fe(C_2O_4)_3]\cdot 3H_2O$ compound (monoclinic $P2_1/c$), which turned out to be isotypic to the reported potassium salt (Junk, 2005; Piro *et al.*, 2016), and the triclinic ($P\overline{1}$) $Rb(C_2O_4H)(C_2O_4H_2)\cdot 2H_2O$ salt (Kherfi *et al.*, 2010), which is isotypic to the ammonium analogue (Jarzembska *et al.*, 2014). A third phase consisted of large green crystals of a new cubic ($P4_332$) $NaRb_5[Fe(C_2O_4)_3]_2$ salt. Interestingly, the isotypic counterpart of this salt where rubi-

Table 1
Bond lengths and angles (Å, °) around iron(III) and within the oxalate dianion in $NaRb_5[Fe(C_2O_4)_3]_2$ $P4_332$ enantiomer.

(*a*) At a crystal site of C_3 point group symmetry.

Iron(III)[a]		$(C_2O_4)^{2-}$			
Fe—O11	2.021 (4)	C1–O12	1.211 (7)	O12—C—O11	125.2 (6)
Fe—O21	1.989 (4)	C1–O11	1.286 (7)	O12—C1—C2	121.2 (6)
		C1—C2	1.540 (9)	O11—C1—C2	113.5 (5)
O21—Fe—O11	80.0 (2)	C2—O22	1.211 (7)	O22—C2—O21	125.3 (6)
O21—Fe—O21^{i}	88.4 (2)	C2—O21	1.283 (7)	O22—C2—C1	121.1 (6)
O11—Fe—O11^{i}	88.7 (2)			O21—C2—C1	113.6 (5)
O11—Fe—O21^{i}	106.2 (2)				
O11—Fe—O21^{ii}	160.9 (2)				

Symmetry codes: (i) $-z+\frac{1}{2}, -x+1, y-\frac{1}{2}$; (ii) $-y+1, z+\frac{1}{2}, -x+\frac{1}{2}$.

dium is replaced by potassium has been reported by Wartchow (1997) to appear in a mixture with crystals of the monoclinic $K_3[Fe(C_2O_4)_3]\cdot 3H_2O$ salt, hence confirming the tendency of potassium and rubidium alkaline ions to form isotypic crystal analogues (Piro *et al.*, 2016). Curiously, in a previous work, Henneicke & Wartchow (1997) reported the chiral counterpart of the cubic $NaK_5[Fe(C_2O_4)_3]_2$ salt, which crystallizes in the space group $P4_132$. This prompted us to search for the chiral rubidium analogue in the very same batch as the single-crystals that solved in the space group $P4_332$ $NaRb_5[Fe(C_2O_4)_3]_2$. By chance, we picked a single crystal and submitted it to X-ray diffraction scrutiny to find that it now belonged to the chiral space group $P4_132$. This strongly suggests that the $NaM_5[Fe(C_2O_4)_3]_2$ (M = K, Rb) crystal samples could be racemic conglomerates generated by spontaneous resolution, a rare event discovered by Louis Pasteur in 1848 (Pasteur, 1848*a*,*b*) in a famous experiment in which he hand-sorted the chirally resolved crystals of sodium ammonium tartrate tetrahydrate on the basis of their observed morphology and then examined their respective solutions with a polarimeter to find opposite rotations of the plane of light polarization (Flack, 2009). Recently, we found that the phenomenon could also have occurred in isotypic $[M(Lap)_2]_n$ (M = Cd, Mn; HLap = 2-hydroxy-3-(3-methyl-2-butenyl)-1,4-naphtoquinone, $C_{15}H_{14}O_3$) complexes whose enantiomers crystallize in the tetragonal and enantiomorphic space groups $P4_32_12$ and $P4_12_12$ (Farfán *et al.*, 2015).

2. Structural commentary

Fig. 1 shows an *ORTEP* (Farrugia, 2012) drawing of the $P4_332$ enantiomer of the title compound. Bond lengths and angles around iron(III) and within the oxalate dianion are listed in Table 1 and contact distances around the alkali ions are shown in Table 2. All metal ions are at crystallographic special positions while the oxalate anion is on a general position. The iron(III) ion is on a threefold axis, C_3 point group symmetry (Wyckoft *c* site), in an octahedral environment (FeO_6 core). It is coordinated to three, symmetry-related, oxalate anions acting as bidentate ligands through the oxygen atoms of their opposite carboxylic groups in a propeller-like conformation and along one electron pair lobe on each oxygen ligand. The FeO_6 bond geometry and metrics are consistent with the oxalate being a weak-field ligand that gives rise to the high-spin (S = 5/2) electronic ground state exhibited by the complex, as probed by magnetic susceptibility (Delgado *et al.*, 2002) and ESR spectroscopy (Collison & Powell, 1990) in synthetic minguzzite, $K_3[Fe(C_2O_4)_3]\cdot 3H_2O$, by polarized electronic absorption spectroscopy in single crystal $NaMg[(Fe,Al)(C_2O_4)_3]\cdot 9H_2O$ mixtures (Piper & Carlin, 1961) and also by

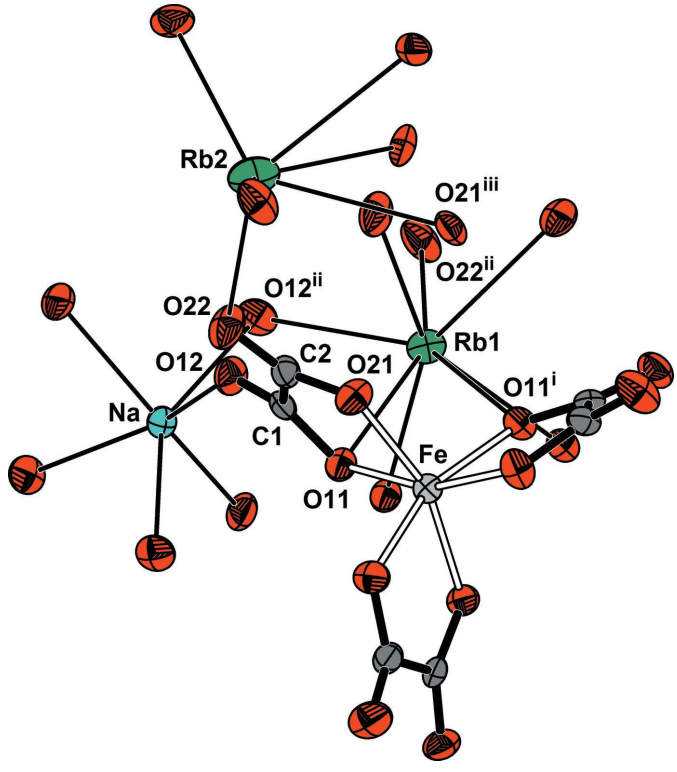

Figure 1
View of $NaRb_5[Fe(C_2O_4)_3]_2$ showing the atom labels and displacement ellipsoids at the 50% probability level. For clarity, only the minimum number of oxygen ligands around each metal ion has been labelled. The rest of the environmental oxygen atoms are generated through the symmetry operations of the corresponding point groups: C_3 (Fe), C_2 (Rb1), C_3 (Rb2) and D_3 (Na). Iron–oxalate bonds are indicated by double lines and alkali metal–oxygen contacts by single lines. Symmetry codes: (i) $-y+1, z+\frac{1}{2}, -x+\frac{1}{2}$; (ii) $y-\frac{1}{2}, -z+\frac{3}{2}, -x+1$; (iii) $-y+\frac{5}{4}, -x+\frac{5}{4}, -z+\frac{1}{4}$.

Table 2
Bond lengths (Å) around the alkali metal ions in $NaRb_5[Fe(C_2O_4)_3]_2$ $P4_332$ enantiomer..

(*a*) At a site of C_2 point group symmetry; (*b*) at a C_3 site; (*c*) at a D_3 site.

Rb1[a]		Rb2[b]		Na[c]	
Rb1—O11	3.009 (4)	Rb2—O22	2.808 (4)	Na—O12	2.439 (4)
Rb1—O11^{i}	3.067 (4)	Rb2—O21^{iii}	3.114 (4)		
Rb1—O22^{ii}	2.788 (5)				
Rb1—O12^{ii}	3.133 (5)				

Symmetry codes: (i) $-y+1, z+\frac{1}{2}, -x+\frac{1}{2}$; (ii) $y-\frac{1}{2}, -z+\frac{3}{2}, -x+1$; (iii) $-y+\frac{5}{4}, -x+\frac{5}{4}, -z+\frac{1}{4}$.

Mössbauer spectroscopy in $K_3[Fe(C_2O_4)_3]\cdot 3H_2O$ (Bancroft *et al.*, 1970; Sato & Tominaga, 1979; Ladriere, 1992) and in the alkali (Na, Rb, Cs) family of tris(oxalato)ferrate(III) salts (Piro *et al.*, 2016).

The planes of the carboxylic $-COO^-$ groups of the oxalate ligand are slightly tilted from each other, by 12 (1)° around the C—C σ-bond. As expected, the C—O bond lengths involving the coordinated-to-metal oxygen atoms are significantly longer [1.286 (7) and 1.283 (7) Å] than the ones corresponding to the uncoordinated oxalate oxygen atoms [both equal to 1.211 (7) Å].

There are two independent rubidium ions, one (Rb1) lying on a twofold axis, C_2 point group symmetry (*d* site) in an eightfold coordination with neighbouring oxalate oxygen atoms, the other one (Rb2) on a threefold axis, C_3 point group (*c* site) in a sixfold coordination. The sodium ion is at a site of D_3 point group symmetry (*a* site) in a trigonal–antiprismatic NaO_6 coordination with one oxygen atom of six neighbouring, symmetry-related, oxalate ions.

When dealing with octahedral $Fe(C_2O_4)_3$ tris-chelated metal complexes, it is customary to describe its chirality employing Λ- and Δ-descriptors (Meierhenrich, 2008). It turns out that the enantiomeric complexes correlate with the corresponding chiral space groups, as indicated in Fig. 2.

The possibility of controlling the crystal chirality and therefore obtaining enhanced optical activity of functional materials has been discussed (Gruselle *et al.*, 2006). To this purpose, two general synthetic routes have been developed to reach optically active coordination compounds, namely either by enantioselective synthesis using enantiopure chiral species, which yields enantiopure samples (Knof & von Zelewsky, 1999) or by spontaneous resolution upon crystallization from a racemate, which yields a conglomerate (Pérez-García & Amabilino, 2002). As explained above, the chiral $NaRb_5[Fe(C_2O_4)_3]_2$ crystals were obtained through the phenomena of spontaneous resolution from a racemic solution of $[Fe(C_2O_4)_3]^{3-}$ complex ions into a racemic conglomerate. This is presumably followed by a structural inductive effect by these chiral molecular ions on the alkali metal ions through shared oxalate ligands. In fact, not only is the Fe^{III} ion a 'stereogenic centre' in the $Fe(C_2O_4)_3$ tris-chelated metal complex, but so also are the sodium and one (Rb2) of the rubidium ions. These metal ions are in a distorted octahedral environment coordinated to six oxalate anions, acting as monodentate ligand through one of their oxygen atoms and resembling a six-bladed propeller-like conformation. From the structural data, it turns out that the chirality of this local arrangement around the alkaline ions is coincident with the one of the $[Fe(C_2O_4)_3]^{3-}$ inductor and therefore the chiral crystals reported here can be more conveniently described as Λ-NaΛ-$Rb_2Rb_3[\Lambda\text{-}Fe(C_2O_4)_3]_2$ ($P4_332$) and Δ-NaΔ-$Rb_2Rb_3[\Delta\text{-}Fe(C_2O_4)_3]_2$ ($P4_132$). However, no definitive chirality can be unambiguously assigned to the other independent rubidium (Rb1) ion which is in an eightfold polyhedral coordination.

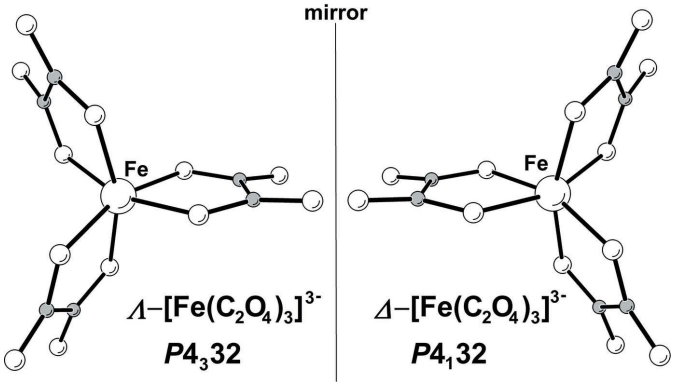

Figure 2
Views of the Λ and Δ enantiomers of $[Fe(C_2O_4)_3]^{3-}$.

3. Database survey

The formation of racemic conglomerates of single crystals, adequate for structural X-ray diffraction, generated by spontaneous resolution is an infrequent phenomenon. In fact, a search of the Cambridge Structural Database (Groom *et al.*, 2016) invoking the term 'spontaneous resolution' showed seventeen entries, and another one using as a target 'chiral crystals' produced a further four hits. Among them there were reported the chiral to each other (*M*)- and (*P*)-*catena*-{[μ_2-2-(imidazo[4,5-*f*](1,10)phenanthrolin-2-yl)benzoato-*N*,*N*′,*O*]-aquachlorozinc(II)} (CSD refcodes EJINOB and EJINUH; Wei *et al.*, 2011) and *catena*-[(μ_8-benzene-1,3,5-tricarboxylato)lithiumzinc] (CSD refcodes WAJHUM and WAJJAU; Xie *et al.*, 2010).

4. Synthesis and crystallization

As stated in the *Chemical context*, in one of the preparations generated during the synthesis of the rubidium salt of $[Fe(C_2O_4)_3]^{3-}$, by reaction of freshly precipitated $Fe(OH)_3$ (obtained by dropwise addition of a small excess of 20% NaOH to an Fe^{III} solution) with rubidium oxalate: $Fe(OH)_3 + 3Rb(HC_2O_4) + 3H_2O \rightarrow Rb_3[Fe(C_2O_4)_3]\cdot 3H_2O + 3H_2O$ (Piro *et al.*, 2016), we found a relatively complex reaction giving rise to a poly-phased crystal mixture, from which the $NaRb_5[Fe(C_2O_4)_3]_2$ chiral pair could be isolated.

Table 3
Experimental details.

	Cubic, $P4_332$	Cubic, $P4_132$
Crystal data		
Chemical formula	$NaRb_5[Fe(C_2O_4)_3]_2$	$NaRb_5[Fe(C_2O_4)_3]_2$
M_r	1090.16	1090.16
Temperature (K)	297	293
a (Å)	13.8058 (4)	13.7995 (3)
V (Å^3)	2631.4 (2)	2627.79 (17)
Z	4	4
Radiation type	Mo $K\alpha$	Mo $K\alpha$
μ (mm^{-1})	10.42	10.43
Crystal size (mm)	0.48 × 0.42 × 0.38	0.48 × 0.35 × 0.25
Data collection		
Diffractometer	Agilent Xcalibur Eos Gemini	Rigaku Oxford Diffraction Xcalibur, Eos, Gemini
Absorption correction	Multi-scan (*CrysAlis PRO*; Agilent, 2014)	Multi-scan (*CrysAlis PRO*; Rigaku OD, 2015)
T_{min}, T_{max}	0.690, 1.000	0.786, 1.000
No. of measured, independent and observed [$I > 2\sigma(I)$] reflections	2960, 959, 767	4284, 961, 814
R_{int}	0.043	0.038
(sin $\theta/\lambda)_{max}$ (Å^{-1})	0.638	0.638
Refinement		
$R[F^2 > 2\sigma(F^2)]$, $wR(F^2)$, S	0.035, 0.064, 1.00	0.032, 0.068, 1.02
No. of reflections	959	961
No. of parameters	68	68
$\Delta\rho_{max}$, $\Delta\rho_{min}$ (e Å^{-3})	0.84, −0.85	1.02, −0.95
Absolute structure	Flack x determined using 225 quotients $[(I^+)-(I^-)]/[(I^+)+(I^-)]$ (Parsons *et al.*, 2013)	Flack x determined using 251 quotients $[(I^+)-(I^-)]/[(I^+)+(I^-)]$ (Parsons *et al.*, 2013).
Absolute structure parameter	−0.013 (12)	−0.003 (10)

Computer programs: *CrysAlis PRO* (Agilent, 2014; Rigaku OD, 2015), *SHELXT* (Sheldrick, 2015*a*), *SHELXL2014* (Sheldrick, 2015*b*) and *ORTEP-3 for Windows* (Farrugia, 2012).

5. Refinement details

Crystal data, data collection procedure and structure refinement results are summarized in Table 3. The structure was solved by intrinsic phasing with *SHELXT* (Sheldrick, 2015*a*). The stereoisomers were determined through refinement of the Flack absolute structure parameter. This is the fractional contribution to the diffraction pattern due to the molecule racemic twin and for the correct enantiomeric crystal it should be zero to within experimental error.

Funding information

Funding for this research was provided by: CONICET (PIP 11220130100651CO) and UNLP (Project 11/X709) of Argentina. OEP and GAE are Research Fellows of CONICET.

References

Agilent (2014). *CrysAlis PRO*. Agilent Technologies Ltd, Yarnton, England.
Bancroft, G. M., Dharmawardena, K. G. & Maddock, A. G. (1970). *Inorg. Chem.* **9**, 223–226.
Coles, H. (1998). *Chiral Nematics: Physical Properties and Applications*. In *Handbook of Liquid Crystals*, Vol. 2A, edited by D. Demus, J. Goodby, G. W. Gray, H. W. Spiess & V. Vill, ch. IV, pp. 335–409. Weinheim: Wiley-VCH.
Collison, D. & Powell, A. K. (1990). *Inorg. Chem.* **29**, 4735–4746.
Coronado, E., Palacio, F. & Veciana, J. (2003). *Angew. Chem. Int. Ed.* **42**, 2570–2572.
Delgado, G., Mora, A. J. & Sagredo, V. (2002). *Physica B*, **320**, 410–412.
Farfán, R. A., Espíndola, J. A., Gómez, M. I., de Jiménez, M. C. L., Piro, O. E., Castellano, E. E. & Martínez, M. A. (2015). *J. Mol. Struct.* **1087**, 80–87.
Farrugia, L. J. (2012). *J. Appl. Cryst.* **45**, 849–854.
Flack, H. D. (2003). *Helv. Chim. Acta*, **86**, 905–921.
Flack, H. D. (2009). *Acta Cryst.* A**65**, 371–389.
Goodby, J. W. (1998). *Symmetry and Chirality in Liquid Crystals*. In *Handbook of Liquid Crystals*, Vol. 1, edited by D. Demus, J. Goodby, G. W. Gray, H. W. Spiess & V. Vill, ch V, pp. 115–132. Weinheim: Wiley-VCH.
Groom, C. R., Bruno, I. J., Lightfoot, M. P. & Ward, S. C. (2016). *Acta Cryst.* B**72**, 171–179.
Gruselle, M., Train, C., Boubekeur, K., Gredin, P. & Ovanesyan, N. (2006). *Coord. Chem. Rev.* **250**, 2491–2500.
Henneicke, S. & Wartchow, R. (1997). *Z. Kristallogr.* **212**, 56.
Jarzembska, K. N., Kamiński, R., Dobrzycki, Ł. & Cyrański, M. K. (2014). *Acta Cryst.* B**70**, 847–855.
Junk, P. C. (2005). *J. Coord. Chem.* **58**, 355–361.
Kherfi, H., Hamadene, M., Guehria-Laidoudi, A., Dahaoui, S. & Lecomte, C. (2010). *Materials* **3**, 1281–1301.
Knof, U. & von Zelewsky, A. (1999). *Angew. Chem. Int. Ed.* **38**, 302–322.
Knowles, W. S. (2001). Nobel lecture: *Asymmetric Hydrogenation*. https://www. nobelprize. org/nobel_prizes/chemistry/laureates/2001/knowles-lecture. pdf
Ladriere, J. (1992). *Hyperfine Interact.* **70**, 1095–1098.
Meierhenrich, U. (2008). *Amino Acids and the Asymmetry of Life*. Berlin: Springer-Verlag.
Nguyen, L. A., He, H. & Pham-Huy, C. (2006). *Int. J. Biomed. Sci.* **2**, 85–100.
Noyori, R. (2001). Nobel lecture: *Asymmetric Catalysis: Science and Opportunities*. https://www. nobelprize. org/nobel_prizes/chemistry/laureates/2001/noyori-lecture. pdf

Parsons, S., Flack, H. D. & Wagner, T. (2013). *Acta Cryst.* B**69**, 249–259.
Pasteur, L. (1848*a*). *C. R. Acad. Sci. Paris*, **26**, 535–538.
Pasteur, L. (1848*b*). *Anal. Chim. Phys.* **24**, 442–459.
Pérez-García, L. & Amabilino, D. B. (2002). *Chem. Soc. Rev*. **31**, 342–356.
Piper, T. S. & Carlin, R. L. (1961). *J. Chem. Phys.* **35**, 1809–1815.
Piro, O. E., Echeverría, G. A., Mercader, R. A., González-Baró, A. C. & Baran, E. J. (2016). *J. Coord. Chem.* **69**, 3715–3725.
Rigaku OD (2014). *CrysAlis PRO*. Rigaku Oxford Diffraction, Yarnton, England.
Sato, H. & Tominaga, T. (1979). *Bull. Chem. Soc. Jpn*, **52**, 1402–1407.
Sharpless, K. B. (2001). Nobel lecture: *Searching for New Reactivity*. https://www. nobelprize. org/nobel_prizes/chemistry/laureates/2001/sharpless-lecture. pdf
Sheldrick, G. M. (2015*a*). *Acta Cryst.* A**71**, 3–8.
Sheldrick, G. M. (2015*b*). *Acta Cryst.* C**71**, 3–8.
Wartchow, R. (1997). *Z. Kristallogr.* **212**, 57.
Wei, Y., Wu, K., He, J., Zheng, W. & Xiao, X. (2011). *CrystEngComm*, **13**, 52–54.
Xie, L.-H., Lin, J.-B., Liu, X.-M., Wang, Y., Zhang, W.-X., Zhang, J.-P. & Chen, X.-M. (2010). *Inorg. Chem.* **49**, 1158–1165.

supporting information

Acta Cryst. (2018). E**74**, 905-909 [https://doi.org/10.1107/S2056989018008022]

Spontaneous enantiomorphism in poly-phased alkaline salts of tris-(oxalato)ferrate(III): crystal structure of cubic $NaRb_5[Fe(C_2O_4)_3]_2$

O. E. Piro, G. A. Echeverría and E. J. Baran

Computing details

Data collection: *CrysAlis PRO* (Agilent, 2014) for P4332; *CrysAlis PRO* (Rigaku OD, 2015) for P4132. Cell refinement: *CrysAlis PRO* (Agilent, 2014) for P4332; *CrysAlis PRO* (Rigaku OD, 2015) for P4132. Data reduction: *CrysAlis PRO* (Agilent, 2014) for P4332; *CrysAlis PRO* (Rigaku OD, 2015) for P4132. For both structures, program(s) used to solve structure: SHELXT (Sheldrick, 2015a); program(s) used to refine structure: *SHELXL2014* (Sheldrick, 2015b); molecular graphics: *ORTEP-3 for Windows* (Farrugia, 2012); software used to prepare material for publication: *SHELXL2014* (Sheldrick, 2015b).

Sodium pentarubidium bis[tris(oxalato)ferrate(III)] (P4332)

Crystal data

$NaRb_5[Fe(C_2O_4)_3]_2$
M_r = 1090.16
Cubic, $P4_332$
a = 13.8058 (4) Å
V = 2631.4 (2) Å^3
Z = 4
$F(000)$ = 2048
D_x = 2.752 Mg m^{-3}
Mo $K\alpha$ radiation, λ = 0.71073 Å
Cell parameters from 922 reflections
θ = 3.6–27.3°
μ = 10.42 mm^{-1}
T = 297 K
Fragment, green
0.48 × 0.42 × 0.38 mm

Data collection

Agilent Xcalibur Eos Gemini diffractometer
Radiation source: Enhance (Mo) X-ray Source
Graphite monochromator
Detector resolution: 16.0604 pixels mm^{-1}
ω scans
Absorption correction: multi-scan (CrysAlis PRO; Agilent, 2014)
T_{min} = 0.690, T_{max} = 1.000
2960 measured reflections
959 independent reflections
767 reflections with $I > 2\sigma(I)$
R_{int} = 0.043
θ_{max} = 27.0°, θ_{min} = 3.3°
h = −8→17
k = −11→16
l = −8→10

Refinement

Refinement on F^2
Least-squares matrix: full
$R[F^2 > 2\sigma(F^2)]$ = 0.035
$wR(F^2)$ = 0.064
S = 1.00
959 reflections
68 parameters
0 restraints
Primary atom site location: dual
$w = 1/[\sigma^2(F_o^2) + (0.0274P)^2]$ where $P = (F_o^2 + 2F_c^2)/3$
$(\Delta/\sigma)_{max} < 0.001$
$\Delta\rho_{max}$ = 0.84 e Å^{-3}
$\Delta\rho_{min}$ = −0.85 e Å^{-3}

Absolute structure: Flack *x* determined using 225 quotients $[(I^+)-(I^-)]/[(I^+)+(I^-)]$ (Parsons *et al.*, 2013)
Absolute structure parameter: −0.013 (12)

Special details

Geometry. All esds (except the esd in the dihedral angle between two l.s. planes) are estimated using the full covariance matrix. The cell esds are taken into account individually in the estimation of esds in distances, angles and torsion angles; correlations between esds in cell parameters are only used when they are defined by crystal symmetry. An approximate (isotropic) treatment of cell esds is used for estimating esds involving l.s. planes.

Fractional atomic coordinates and isotropic or equivalent isotropic displacement parameters (Å²)

	x	*y*	*z*	U_{iso}*/U_{eq}
C1	0.3861 (5)	0.8068 (4)	0.3863 (5)	0.0207 (13)
C2	0.4510 (5)	0.7715 (5)	0.3027 (5)	0.0234 (16)
O11	0.2953 (3)	0.7918 (3)	0.3718 (3)	0.0241 (10)
O12	0.4203 (3)	0.8466 (3)	0.4566 (3)	0.0312 (11)
O21	0.4037 (3)	0.7481 (3)	0.2262 (3)	0.0287 (10)
O22	0.5380 (3)	0.7665 (4)	0.3119 (3)	0.0402 (13)
Fe	0.26048 (6)	0.73952 (6)	0.23952 (6)	0.0209 (4)
Rb1	0.25612 (5)	1.00612 (5)	0.3750	0.0290 (3)
Rb2	0.67150 (6)	0.82850 (6)	0.17150 (6)	0.0444 (4)
Na	0.3750	0.8750	0.6250	0.0218 (13)

Atomic displacement parameters (Å²)

	U^{11}	U^{22}	U^{33}	U^{12}	U^{13}	U^{23}
C1	0.025 (3)	0.020 (3)	0.017 (3)	−0.001 (3)	−0.001 (3)	0.006 (3)
C2	0.021 (3)	0.029 (4)	0.020 (3)	0.002 (3)	0.000 (3)	0.004 (3)
O11	0.020 (2)	0.032 (3)	0.020 (2)	0.000 (2)	0.002 (2)	0.000 (2)
O12	0.034 (3)	0.041 (3)	0.019 (2)	−0.003 (2)	−0.004 (2)	−0.002 (2)
O21	0.023 (2)	0.044 (3)	0.019 (2)	−0.004 (2)	0.006 (2)	−0.006 (2)
O22	0.020 (2)	0.069 (4)	0.032 (3)	0.004 (3)	0.003 (2)	0.002 (3)
Fe	0.0209 (4)	0.0209 (4)	0.0209 (4)	−0.0006 (4)	−0.0006 (4)	0.0006 (4)
Rb1	0.0290 (3)	0.0290 (3)	0.0288 (5)	−0.0018 (5)	0.0051 (3)	−0.0051 (3)
Rb2	0.0444 (4)	0.0444 (4)	0.0444 (4)	−0.0115 (4)	0.0115 (4)	−0.0115 (4)
Na	0.0218 (13)	0.0218 (13)	0.0218 (13)	0.0014 (16)	−0.0014 (16)	−0.0014 (16)

Geometric parameters (Å, º)

C1—O12	1.211 (7)	Rb1—O22^{v}	2.788 (5)
C1—O11	1.286 (7)	Rb1—O22^{vi}	2.788 (5)
C1—C2	1.540 (9)	Rb1—O11^{vii}	3.009 (4)
C2—O22	1.211 (7)	Rb1—O11^{iv}	3.067 (4)
C2—O21	1.283 (7)	Rb1—O11^{viii}	3.067 (4)
O11—Fe	2.021 (4)	Rb1—O12^{v}	3.133 (5)
O11—Rb1	3.009 (4)	Rb1—O12^{vi}	3.133 (5)
O11—Rb1^{i}	3.067 (4)	Rb1—O12^{vii}	3.354 (5)

O12—Na	2.439 (4)	Rb2—O22^{ix}	2.808 (4)
O12—Rb1^{ii}	3.133 (5)	Rb2—O22^{x}	2.808 (4)
O12—Rb1	3.354 (5)	Rb2—O21^{iii}	3.114 (4)
O21—Fe	1.989 (4)	Rb2—O21^{xi}	3.114 (4)
O21—Rb2^{iii}	3.114 (4)	Rb2—O21^{vi}	3.114 (4)
O22—Rb1^{ii}	2.788 (5)	Na—O12^{xii}	2.439 (4)
O22—Rb2	2.808 (4)	Na—O12^{ii}	2.439 (4)
Fe—O21^{iv}	1.989 (4)	Na—O12^{xiii}	2.439 (4)
Fe—O21^{i}	1.989 (4)	Na—O12^{viii}	2.439 (4)
Fe—O11^{i}	2.021 (4)	Na—O12^{v}	2.439 (4)
Fe—O11^{iv}	2.021 (4)		

O12—C1—O11	125.2 (6)	O11^{vii}—Rb1—O12^{v}	110.45 (11)
O12—C1—C2	121.2 (6)	O11^{iv}—Rb1—O12^{v}	151.29 (11)
O11—C1—C2	113.5 (5)	O11^{viii}—Rb1—O12^{v}	65.47 (11)
O22—C2—O21	125.3 (6)	O22^{v}—Rb1—O12^{vi}	91.18 (12)
O22—C2—C1	121.1 (6)	O22^{vi}—Rb1—O12^{vi}	56.14 (12)
O21—C2—C1	113.6 (5)	O11—Rb1—O12^{vi}	110.45 (11)
C1—O11—Fe	115.5 (4)	O11^{vii}—Rb1—O12^{vi}	95.92 (11)
C1—O11—Rb1	90.8 (3)	O11^{iv}—Rb1—O12^{vi}	65.47 (11)
Fe—O11—Rb1	108.75 (16)	O11^{viii}—Rb1—O12^{vi}	151.29 (11)
C1—O11—Rb1^{i}	133.5 (4)	O12^{v}—Rb1—O12^{vi}	133.07 (16)
Fe—O11—Rb1^{i}	106.67 (16)	O22^{v}—Rb1—O12^{vii}	64.52 (12)
Rb1—O11—Rb1^{i}	93.73 (11)	O22^{vi}—Rb1—O12^{vii}	114.33 (13)
C1—O12—Na	137.5 (4)	O11—Rb1—O12^{vii}	141.04 (11)
C1—O12—Rb1^{ii}	107.6 (4)	O11^{vii}—Rb1—O12^{vii}	40.34 (11)
Na—O12—Rb1^{ii}	97.96 (14)	O11^{iv}—Rb1—O12^{vii}	90.55 (10)
C1—O12—Rb1	76.5 (4)	O11^{viii}—Rb1—O12^{vii}	90.35 (11)
Na—O12—Rb1	92.39 (13)	O12^{v}—Rb1—O12^{vii}	116.99 (13)
Rb1^{ii}—O12—Rb1	157.89 (15)	O12^{vi}—Rb1—O12^{vii}	62.32 (15)
C2—O21—Fe	116.4 (4)	O22^{v}—Rb1—O12	114.33 (14)
C2—O21—Rb2^{iii}	133.5 (4)	O22^{vi}—Rb1—O12	64.52 (12)
Fe—O21—Rb2^{iii}	95.43 (15)	O11—Rb1—O12	40.34 (11)
C2—O22—Rb1^{ii}	121.7 (4)	O11^{vii}—Rb1—O12	141.04 (11)
C2—O22—Rb2	124.2 (4)	O11^{iv}—Rb1—O12	90.35 (11)
Rb1^{ii}—O22—Rb2	110.80 (17)	O11^{viii}—Rb1—O12	90.55 (10)
O21^{iv}—Fe—O21^{i}	88.42 (18)	O12^{v}—Rb1—O12	62.32 (15)
O21^{iv}—Fe—O21	88.43 (18)	O12^{vi}—Rb1—O12	116.99 (13)
O21^{i}—Fe—O21	88.42 (18)	O12^{vii}—Rb1—O12	178.45 (16)
O21^{iv}—Fe—O11	160.91 (17)	O22^{ix}—Rb2—O22^{x}	116.27 (7)
O21^{i}—Fe—O11	106.20 (17)	O22^{ix}—Rb2—O22	116.27 (7)
O21—Fe—O11	79.96 (16)	O22^{x}—Rb2—O22	116.27 (7)
O21^{iv}—Fe—O11^{i}	106.20 (17)	O22^{ix}—Rb2—O21^{iii}	131.79 (14)
O21^{i}—Fe—O11^{i}	79.96 (16)	O22^{x}—Rb2—O21^{iii}	81.60 (13)
O21—Fe—O11^{i}	160.91 (17)	O22—Rb2—O21^{iii}	89.01 (12)
O11—Fe—O11^{i}	88.73 (17)	O22^{ix}—Rb2—O21^{xi}	81.60 (13)
O21^{iv}—Fe—O11^{iv}	79.96 (16)	O22^{x}—Rb2—O21^{xi}	89.01 (12)
O21^{i}—Fe—O11^{iv}	160.91 (17)	O22—Rb2—O21^{xi}	131.79 (14)

O21—Fe—O11^{iv}	106.20 (17)	O21^{iii}—Rb2—O21^{xi}	52.88 (13)
O11—Fe—O11^{iv}	88.72 (17)	O22^{ix}—Rb2—O21^{vi}	89.01 (12)
O11^{i}—Fe—O11^{iv}	88.73 (17)	O22^{x}—Rb2—O21^{vi}	131.79 (14)
O22^{v}—Rb1—O22^{vi}	95.3 (2)	O22—Rb2—O21^{vi}	81.60 (13)
O22^{v}—Rb1—O11	152.05 (12)	O21^{iii}—Rb2—O21^{vi}	52.88 (13)
O22^{vi}—Rb1—O11	83.24 (13)	O21^{xi}—Rb2—O21^{vi}	52.88 (13)
O22^{v}—Rb1—O11^{vii}	83.24 (13)	O12—Na—O12^{xii}	76.1 (2)
O22^{vi}—Rb1—O11^{vii}	152.05 (12)	O12—Na—O12^{ii}	87.13 (15)
O11—Rb1—O11^{vii}	110.74 (16)	O12^{xii}—Na—O12^{ii}	120.9 (2)
O22^{v}—Rb1—O11^{iv}	152.40 (12)	O12—Na—O12^{xiii}	145.7 (2)
O22^{vi}—Rb1—O11^{iv}	83.98 (12)	O12^{xii}—Na—O12^{xiii}	87.13 (15)
O11—Rb1—O11^{iv}	55.43 (15)	O12^{ii}—Na—O12^{xiii}	76.1 (2)
O11^{vii}—Rb1—O11^{iv}	84.73 (11)	O12—Na—O12^{viii}	120.9 (2)
O22^{v}—Rb1—O11^{viii}	83.98 (12)	O12^{xii}—Na—O12^{viii}	87.13 (15)
O22^{vi}—Rb1—O11^{viii}	152.40 (12)	O12^{ii}—Na—O12^{viii}	145.7 (2)
O11—Rb1—O11^{viii}	84.73 (11)	O12^{xiii}—Na—O12^{viii}	87.13 (15)
O11^{vii}—Rb1—O11^{viii}	55.43 (15)	O12—Na—O12^{v}	87.13 (15)
O11^{iv}—Rb1—O11^{viii}	109.10 (16)	O12^{xii}—Na—O12^{v}	145.7 (2)
O22^{v}—Rb1—O12^{v}	56.14 (12)	O12^{ii}—Na—O12^{v}	87.13 (15)
O22^{vi}—Rb1—O12^{v}	91.18 (12)	O12^{xiii}—Na—O12^{v}	120.9 (2)
O11—Rb1—O12^{v}	95.93 (11)	O12^{viii}—Na—O12^{v}	76.1 (2)

O12—C1—C2—O22	13.4 (10)	Rb1^{ii}—C1—O11—Rb1^{i}	44.6 (12)
O11—C1—C2—O22	−168.2 (6)	O11—C1—O12—Na	24.7 (10)
Rb1—C1—C2—O22	115.8 (6)	C2—C1—O12—Na	−157.1 (4)
Rb1^{ii}—C1—C2—O22	−14.0 (6)	Rb1—C1—O12—Na	78.5 (5)
O12—C1—C2—O21	−167.4 (6)	Rb1^{ii}—C1—O12—Na	−124.1 (6)
O11—C1—C2—O21	11.0 (8)	O11—C1—O12—Rb1^{ii}	148.8 (5)
Rb1—C1—C2—O21	−65.0 (7)	C2—C1—O12—Rb1^{ii}	−32.9 (6)
Rb1^{ii}—C1—C2—O21	165.3 (5)	Rb1—C1—O12—Rb1^{ii}	−157.41 (18)
O12—C1—C2—Rb1^{ii}	27.3 (5)	O11—C1—O12—Rb1	−53.8 (6)
O11—C1—C2—Rb1^{ii}	−154.2 (5)	C2—C1—O12—Rb1	124.5 (6)
Rb1—C1—C2—Rb1^{ii}	129.8 (3)	Rb1^{ii}—C1—O12—Rb1	157.41 (18)
O12—C1—C2—Rb2	−33.2 (10)	O22—C2—O21—Fe	168.6 (6)
O11—C1—C2—Rb2	145.2 (5)	C1—C2—O21—Fe	−10.6 (7)
Rb1—C1—C2—Rb2	69.2 (7)	Rb1^{ii}—C2—O21—Fe	124.4 (11)
Rb1^{ii}—C1—C2—Rb2	−60.5 (5)	Rb2—C2—O21—Fe	−164.6 (2)
O12—C1—O11—Fe	172.3 (5)	O22—C2—O21—Rb2^{iii}	40.5 (10)
C2—C1—O11—Fe	−6.1 (6)	C1—C2—O21—Rb2^{iii}	−138.7 (4)
Rb1—C1—O11—Fe	111.3 (3)	Rb1^{ii}—C2—O21—Rb2^{iii}	−3.7 (16)
Rb1^{ii}—C1—O11—Fe	−108.2 (9)	Rb2—C2—O21—Rb2^{iii}	67.3 (5)
O12—C1—O11—Rb1	61.0 (6)	O21—C2—O22—Rb1^{ii}	−158.0 (5)
C2—C1—O11—Rb1	−117.4 (4)	C1—C2—O22—Rb1^{ii}	21.1 (9)
Rb1^{ii}—C1—O11—Rb1	140.5 (9)	Rb2—C2—O22—Rb1^{ii}	157.4 (7)
O12—C1—O11—Rb1^{i}	−34.9 (9)	O21—C2—O22—Rb2	44.5 (9)

C2—C1—O11—Rb1^{i}	146.7 (4)	C1—C2—O22—Rb2	−136.3 (5)
Rb1—C1—O11—Rb1^{i}	−95.9 (4)		

Symmetry codes: (i) −*z*+1/2, −*x*+1, *y*−1/2; (ii) −*z*+1, *x*+1/2, −*y*+3/2; (iii) −*y*+5/4, −*x*+5/4, −*z*+1/4; (iv) −*y*+1, *z*+1/2, −*x*+1/2; (v) *y*−1/2, −*z*+3/2, −*x*+1; (vi) −*z*+3/4, *y*+1/4, *x*−1/4; (vii) *y*−3/4, *x*+3/4, −*z*+3/4; (viii) *z*−1/4, −*y*+7/4, *x*+1/4; (ix) *z*+1/2, −*x*+3/2, −*y*+1; (x) −*y*+3/2, −*z*+1, *x*−1/2; (xi) *x*+1/4, *z*+3/4, −*y*+3/4; (xii) −*x*+3/4, *z*+1/4, *y*−1/4; (xiii) −*y*+5/4, −*x*+5/4, −*z*+5/4.

sodium and rubidium tris(oxalate)ferrate(III) (P4132)

Crystal data

$NaRb_5[Fe(C_2O_4)_3]_2$
M_r = 1090.16
Cubic, $P4_132$
a = 13.7995 (3) Å
V = 2627.79 (17) Å^3
Z = 4
$F(000)$ = 2048
D_x = 2.756 Mg m^{-3}

Mo $K\alpha$ radiation, λ = 0.71073 Å
Cell parameters from 1328 reflections
θ = 4.4–27.3°
μ = 10.43 mm^{-1}
T = 293 K
Fragment, green
0.48 × 0.35 × 0.25 mm

Data collection

Rigaku Oxford Diffraction Xcalibur, Eos, Gemini diffractometer
Radiation source: fine-focus sealed X-ray tube, Enhance (Mo) X-ray Source
Graphite monochromator
Detector resolution: 16.0604 pixels mm^{-1}
ω scans
Absorption correction: multi-scan (CrysAlisPro; Rigaku OD, 2015)

T_{min} = 0.786, T_{max} = 1.000
4284 measured reflections
961 independent reflections
814 reflections with $I > 2\sigma(I)$
R_{int} = 0.038
θ_{max} = 27.0°, θ_{min} = 3.3°
h = −14→16
k = −14→10
l = −17→16

Refinement

Refinement on F^2
Least-squares matrix: full
$R[F^2 > 2\sigma(F^2)]$ = 0.032
$wR(F^2)$ = 0.068
S = 1.02
961 reflections
68 parameters
0 restraints
Primary atom site location: dual

$w = 1/[\sigma^2(F_o^2) + (0.031P)^2 + 3.9422P]$ where $P = (F_o^2 + 2F_c^2)/3$
$(\Delta/\sigma)_{max} < 0.001$
$\Delta\rho_{max}$ = 1.02 e Å^{-3}
$\Delta\rho_{min}$ = −0.95 e Å^{-3}
Absolute structure: Flack x determined using 251 quotients $[(I^+)-(I^-)]/[(I^+)+(I^-)]$ (Parsons *et al.*, 2013).
Absolute structure parameter: −0.003 (10)

Special details

Geometry. All esds (except the esd in the dihedral angle between two l.s. planes) are estimated using the full covariance matrix. The cell esds are taken into account individually in the estimation of esds in distances, angles and torsion angles; correlations between esds in cell parameters are only used when they are defined by crystal symmetry. An approximate (isotropic) treatment of cell esds is used for estimating esds involving l.s. planes.

Fractional atomic coordinates and isotropic or equivalent isotropic displacement parameters (Å^2)

	x	y	z	U_{iso}*/U_{eq}
C1	0.1366 (5)	0.5569 (4)	0.1362 (5)	0.0228 (14)
C2	0.0522 (5)	0.5213 (5)	0.2007 (5)	0.0256 (15)
O11	0.1218 (3)	0.5418 (3)	0.0448 (3)	0.0254 (10)
O12	−0.0240 (3)	0.4977 (3)	0.1533 (3)	0.0291 (10)

O21	0.2066 (3)	0.5967 (3)	0.1708 (3)	0.0327 (11)
O22	0.0621 (4)	0.5170 (4)	0.2882 (4)	0.0422 (14)
Fe	−0.01047 (6)	0.48953 (6)	0.01047 (6)	0.0218 (4)
Rb1	0.24391 (5)	0.50609 (5)	0.3750	0.0291 (2)
Rb2	−0.07858 (6)	0.57858 (6)	0.42142 (6)	0.0451 (4)
Na	0.3750	0.6250	0.1250	0.0234 (12)

Atomic displacement parameters (Å²)

	U^{11}	U^{22}	U^{33}	U^{12}	U^{13}	U^{23}
C1	0.018 (3)	0.024 (3)	0.027 (4)	0.007 (3)	−0.001 (3)	0.001 (3)
C2	0.026 (4)	0.034 (4)	0.017 (3)	0.006 (3)	0.003 (3)	−0.001 (3)
O11	0.023 (2)	0.032 (3)	0.022 (3)	−0.003 (2)	0.002 (2)	−0.0003 (18)
O12	0.020 (2)	0.042 (3)	0.025 (3)	−0.005 (2)	0.0052 (18)	−0.005 (2)
O21	0.022 (3)	0.041 (3)	0.036 (3)	−0.003 (2)	−0.005 (2)	0.000 (2)
O22	0.032 (3)	0.069 (4)	0.025 (3)	−0.001 (3)	0.003 (2)	0.002 (3)
Fe	0.0218 (4)	0.0218 (4)	0.0218 (4)	0.0003 (4)	−0.0003 (4)	−0.0003 (4)
Rb1	0.0292 (3)	0.0292 (3)	0.0290 (5)	0.0020 (4)	−0.0047 (3)	−0.0047 (3)
Rb2	0.0451 (4)	0.0451 (4)	0.0451 (4)	−0.0124 (4)	0.0124 (4)	−0.0124 (4)
Na	0.0234 (12)	0.0234 (12)	0.0234 (12)	−0.0014 (15)	−0.0014 (15)	0.0014 (15)

Geometric parameters (Å, º)

C1—O21	1.210 (7)	Rb1—O22^{vi}	2.785 (5)
C1—O11	1.295 (8)	Rb1—O11^{vii}	3.006 (4)
C1—C2	1.546 (9)	Rb1—O11^{viii}	3.006 (4)
C2—O22	1.216 (8)	Rb1—O11^{ix}	3.059 (4)
C2—O12	1.280 (7)	Rb1—O11^{x}	3.059 (4)
O11—Fe	2.019 (4)	Rb1—O21^{vi}	3.125 (5)
O11—Rb1^{i}	3.006 (4)	Rb1—O21^{viii}	3.357 (5)
O11—Rb1^{ii}	3.059 (4)	Rb1—O21^{vii}	3.357 (5)
O12—Fe	1.983 (4)	Rb2—O22^{xi}	2.805 (5)
O12—Rb2^{iii}	3.106 (4)	Rb2—O22^{xii}	2.805 (5)
O21—Na	2.439 (4)	Rb2—O12^{xiii}	3.106 (4)
O21—Rb1	3.125 (5)	Rb2—O12^{xiv}	3.106 (4)
O21—Rb1^{i}	3.357 (5)	Rb2—O12^{xv}	3.106 (4)
O22—Rb1	2.785 (5)	Na—O21^{vii}	2.439 (4)
O22—Rb2	2.805 (5)	Na—O21^{x}	2.439 (4)
Fe—O12^{iv}	1.983 (4)	Na—O21^{xvi}	2.439 (4)
Fe—O12^{v}	1.983 (4)	Na—O21^{i}	2.439 (4)
Fe—O11^{v}	2.019 (4)	Na—O21^{xvii}	2.439 (4)
Fe—O11^{iv}	2.019 (4)		
O21—C1—O11	125.7 (6)	O11^{viii}—Rb1—O11^{x}	55.34 (16)
O21—C1—C2	121.2 (6)	O11^{ix}—Rb1—O11^{x}	108.96 (17)
O11—C1—C2	113.0 (5)	O22^{vi}—Rb1—O21^{vi}	56.08 (13)
O21—C1—Rb1^{i}	82.8 (4)	O22—Rb1—O21^{vi}	91.06 (13)
O11—C1—Rb1^{i}	66.1 (3)	O11^{vii}—Rb1—O21^{vi}	110.57 (12)

C2—C1—Rb1^{i}	123.0 (4)	O11^{viii}—Rb1—O21^{vi}	95.97 (11)
O21—C1—Rb1	53.9 (3)	O11^{ix}—Rb1—O21^{vi}	65.63 (12)
O11—C1—Rb1	154.8 (4)	O11^{x}—Rb1—O21^{vi}	151.23 (11)
C2—C1—Rb1	74.1 (3)	O22^{vi}—Rb1—O21	91.06 (13)
Rb1^{i}—C1—Rb1	131.92 (18)	O22—Rb1—O21	56.09 (13)
O22—C2—O12	125.9 (6)	O11^{vii}—Rb1—O21	95.97 (11)
O22—C2—C1	120.2 (6)	O11^{viii}—Rb1—O21	110.57 (12)
O12—C2—C1	113.9 (5)	O11^{ix}—Rb1—O21	151.23 (11)
O22—C2—Rb1	41.2 (3)	O11^{x}—Rb1—O21	65.63 (12)
O12—C2—Rb1	159.2 (4)	O21^{vi}—Rb1—O21	132.93 (17)
C1—C2—Rb1	81.3 (3)	O22^{vi}—Rb1—O21^{viii}	114.16 (14)
O22—C2—Rb2	39.9 (3)	O22—Rb1—O21^{viii}	64.53 (13)
O12—C2—Rb2	94.4 (4)	O11^{vii}—Rb1—O21^{viii}	141.04 (12)
C1—C2—Rb2	142.1 (4)	O11^{viii}—Rb1—O21^{viii}	40.54 (11)
Rb1—C2—Rb2	79.41 (13)	O11^{ix}—Rb1—O21^{viii}	90.67 (11)
C1—O11—Fe	115.3 (4)	O11^{x}—Rb1—O21^{viii}	90.36 (11)
C1—O11—Rb1^{i}	90.7 (3)	O21^{vi}—Rb1—O21^{viii}	62.26 (16)
Fe—O11—Rb1^{i}	108.83 (17)	O21—Rb1—O21^{viii}	116.94 (14)
C1—O11—Rb1^{ii}	133.3 (4)	C1^{vii}—Rb1—O21^{viii}	160.09 (13)
Fe—O11—Rb1^{ii}	106.92 (16)	C1^{viii}—Rb1—O21^{viii}	20.95 (13)
Rb1^{i}—O11—Rb1^{ii}	93.89 (12)	O22^{vi}—Rb1—O21^{vii}	64.53 (13)
C2—O12—Fe	116.4 (4)	O22—Rb1—O21^{vii}	114.16 (14)
C2—O12—Rb2^{iii}	133.5 (4)	O11^{vii}—Rb1—O21^{vii}	40.54 (11)
Fe—O12—Rb2^{iii}	95.68 (16)	O11^{viii}—Rb1—O21^{vii}	141.04 (12)
C1—O21—Na	137.0 (4)	O11^{ix}—Rb1—O21^{vii}	90.36 (11)
C1—O21—Rb1	107.8 (4)	O11^{x}—Rb1—O21^{vii}	90.67 (11)
Na—O21—Rb1	98.10 (14)	O21^{vi}—Rb1—O21^{vii}	116.94 (14)
C1—O21—Rb1^{i}	76.2 (4)	O21—Rb1—O21^{vii}	62.26 (16)
Na—O21—Rb1^{i}	92.25 (14)	C1^{vii}—Rb1—O21^{vii}	20.95 (13)
Rb1—O21—Rb1^{i}	158.07 (17)	C1^{viii}—Rb1—O21^{vii}	160.09 (13)
C2—O22—Rb1	122.0 (4)	O21^{viii}—Rb1—O21^{vii}	178.23 (16)
C2—O22—Rb2	124.0 (5)	O22—Rb2—O22^{xi}	116.26 (7)
Rb1—O22—Rb2	110.97 (18)	O22—Rb2—O22^{xii}	116.26 (7)
O12—Fe—O12^{iv}	88.19 (18)	O22^{xi}—Rb2—O22^{xii}	116.26 (7)
O12—Fe—O12^{v}	88.19 (18)	O22—Rb2—O12^{xiii}	89.16 (13)
O12^{iv}—Fe—O12^{v}	88.19 (18)	O22^{xi}—Rb2—O12^{xiii}	131.71 (15)
O12—Fe—O11^{v}	161.01 (17)	O22^{xii}—Rb2—O12^{xiii}	81.59 (14)
O12^{iv}—Fe—O11^{v}	106.36 (18)	O22—Rb2—O12^{xiv}	131.71 (15)
O12^{v}—Fe—O11^{v}	80.31 (17)	O22^{xi}—Rb2—O12^{xiv}	81.59 (14)
O12—Fe—O11^{iv}	106.35 (18)	O22^{xii}—Rb2—O12^{xiv}	89.16 (13)
O12^{iv}—Fe—O11^{iv}	80.31 (17)	O12^{xiii}—Rb2—O12^{xiv}	52.74 (13)
O12^{v}—Fe—O11^{iv}	161.01 (17)	O22—Rb2—O12^{xv}	81.59 (14)
O11^{v}—Fe—O11^{iv}	88.44 (18)	O22^{xi}—Rb2—O12^{xv}	89.16 (13)
O12—Fe—O11	80.31 (17)	O22^{xii}—Rb2—O12^{xv}	131.71 (15)
O12^{iv}—Fe—O11	161.01 (17)	O12^{xiii}—Rb2—O12^{xv}	52.74 (13)
O12^{v}—Fe—O11	106.36 (18)	O12^{xiv}—Rb2—O12^{xv}	52.74 (13)
O11^{v}—Fe—O11	88.43 (18)	O21—Na—O21^{vii}	86.98 (16)
O11^{iv}—Fe—O11	88.43 (18)	O21—Na—O21^{x}	76.2 (2)

O22^{vi}—Rb1—O22	95.0 (2)	O21^{vii}—Na—O21^{x}	121.3 (2)
O22^{vi}—Rb1—O11^{vii}	83.52 (14)	O21—Na—O21^{xvi}	145.5 (2)
O22—Rb1—O11^{vii}	152.04 (13)	O21^{vii}—Na—O21^{xvi}	76.2 (2)
O22^{vi}—Rb1—O11^{viii}	152.04 (13)	O21^{x}—Na—O21^{xvi}	86.97 (16)
O22—Rb1—O11^{viii}	83.52 (14)	O21—Na—O21^{i}	86.97 (16)
O11^{vii}—Rb1—O11^{viii}	110.46 (16)	O21^{vii}—Na—O21^{i}	86.97 (16)
O22^{vi}—Rb1—O11^{ix}	84.14 (13)	O21^{x}—Na—O21^{i}	145.5 (2)
O22—Rb1—O11^{ix}	152.50 (13)	O21^{xvi}—Na—O21^{i}	121.3 (2)
O11^{vii}—Rb1—O11^{ix}	55.34 (16)	O21—Na—O21^{xvii}	121.3 (2)
O11^{viii}—Rb1—O11^{ix}	84.61 (12)	O21^{vii}—Na—O21^{xvii}	145.5 (2)
O22^{vi}—Rb1—O11^{x}	152.49 (13)	O21^{x}—Na—O21^{xvii}	86.97 (16)
O22—Rb1—O11^{x}	84.14 (13)	O21^{xvi}—Na—O21^{xvii}	86.97 (16)
O11^{vii}—Rb1—O11^{x}	84.61 (12)	O21^{i}—Na—O21^{xvii}	76.2 (2)

O21—C1—C2—O22	−13.0 (10)	Rb1—C1—O11—Rb1^{ii}	−44.8 (12)
O11—C1—C2—O22	168.7 (6)	O22—C2—O12—Fe	−169.1 (6)
Rb1^{i}—C1—C2—O22	−115.7 (6)	C1—C2—O12—Fe	10.3 (7)
Rb1—C1—C2—O22	14.4 (6)	Rb1—C2—O12—Fe	−124.2 (11)
O21—C1—C2—O12	167.5 (6)	Rb2—C2—O12—Fe	164.4 (2)
O11—C1—C2—O12	−10.8 (8)	O22—C2—O12—Rb2^{iii}	−40.6 (10)
Rb1^{i}—C1—C2—O12	64.8 (6)	C1—C2—O12—Rb2^{iii}	138.9 (4)
Rb1—C1—C2—O12	−165.1 (5)	Rb1—C2—O12—Rb2^{iii}	4.4 (16)
O21—C1—C2—Rb1	−27.4 (5)	Rb2—C2—O12—Rb2^{iii}	−67.1 (5)
O11—C1—C2—Rb1	154.3 (5)	O11—C1—O21—Na	−24.5 (10)
Rb1^{i}—C1—C2—Rb1	−130.1 (3)	C2—C1—O21—Na	157.3 (4)
O21—C1—C2—Rb2	32.8 (10)	Rb1^{i}—C1—O21—Na	−78.2 (5)
O11—C1—C2—Rb2	−145.6 (5)	Rb1—C1—O21—Na	124.2 (6)
Rb1^{i}—C1—C2—Rb2	−69.9 (7)	O11—C1—O21—Rb1	−148.7 (5)
Rb1—C1—C2—Rb2	60.1 (5)	C2—C1—O21—Rb1	33.2 (6)
O21—C1—O11—Fe	−172.2 (5)	Rb1^{i}—C1—O21—Rb1	157.58 (19)
C2—C1—O11—Fe	6.0 (6)	O11—C1—O21—Rb1^{i}	53.7 (6)
Rb1^{i}—C1—O11—Fe	−111.3 (3)	C2—C1—O21—Rb1^{i}	−124.4 (6)
Rb1—C1—O11—Fe	107.9 (9)	Rb1—C1—O21—Rb1^{i}	−157.58 (19)
O21—C1—O11—Rb1^{i}	−60.9 (6)	O12—C2—O22—Rb1	157.6 (5)
C2—C1—O11—Rb1^{i}	117.3 (4)	C1—C2—O22—Rb1	−21.9 (8)
Rb1—C1—O11—Rb1^{i}	−140.8 (9)	Rb2—C2—O22—Rb1	−158.5 (8)
O21—C1—O11—Rb1^{ii}	35.0 (9)	O12—C2—O22—Rb2	−43.9 (9)
C2—C1—O11—Rb1^{ii}	−146.7 (4)	C1—C2—O22—Rb2	136.6 (5)
Rb1^{i}—C1—O11—Rb1^{ii}	96.0 (4)	Rb1—C2—O22—Rb2	158.5 (8)

Symmetry codes: (i) −*z*+1/2, −*x*+1, *y*−1/2; (ii) −*x*+1/2, −*y*+1, *z*−1/2; (iii) *y*−3/4, −*x*+1/4, *z*−1/4; (iv) −*z*, *x*+1/2, −*y*+1/2; (v) *y*−1/2, −*z*+1/2, −*x*; (vi) −*y*+3/4, −*x*+3/4, −*z*+3/4; (vii) −*y*+1, *z*+1/2, −*x*+1/2; (viii) −*z*+1/4, *y*−1/4, *x*+1/4; (ix) −*x*+1/2, −*y*+1, *z*+1/2; (x) *y*−1/4, *x*+1/4, −*z*+1/4; (xi) −*y*+1/2, −*z*+1, *x*+1/2; (xii) *z*−1/2, −*x*+1/2, −*y*+1; (xiii) −*x*−1/4, −*z*+3/4, −*y*+3/4; (xiv) −*y*+1/4, *x*+3/4, *z*+1/4; (xv) *z*−1/4, *y*+1/4, −*x*+1/4; (xvi) −*x*+3/4, −*z*+3/4, −*y*+3/4; (xvii) *z*+1/4, −*y*+5/4, *x*−1/4.